Latin American Journal of Solids and Structures
www.lajss.org

Thermo-mechanical vibration analysis of annular and circular graphene sheet embedded in an elastic medium

Abstract

In this study, the vibration behavior of annular and circular graphene sheet coupled with temperature change and under in-plane pre-stressed is studied. Influence of the surrounding elastic medium on the fundamental frequencies of the single-layered graphene sheets (SLGSs) is investigated. Both Winkler-type and Pasternak-type models are employed to simulate the interaction of the graphene sheets with a surrounding elastic medium. By using the nonlocal elasticity theory the governing equation is derived for SLGSs. The closed-form solution for frequency vibration of circular graphene sheets has been obtained and nonlocal parameter, in-plane pre-stressed, the parameters of elastic medium and temperature change appears into arguments of Bessel functions. The results are subsequently compared with valid result reported in the literature and the molecular dynamics (MD) results. The effects of the small scale, pre-stressed, mode number, temperature change, elastic medium and boundary conditions on natural frequencies are investigated. The non-dimensional frequency decreases at high temperature case with increasing the temperature change for all boundary conditions. The effect of temperature change on the frequency vibration becomes the opposite at high temperature case in compression with the low temperature case. The present research work thus reveals that the nonlocal parameter, boundary conditions and temperature change have significant effects on vibration response of the circular nanoplates. The present results can be used for the design of the next generation of nanodevices that make use of the thermal vibration properties of the graphene.

Keywords

Vibration, In-plane pre-stressed, Circular and annular graphene sheet, Temperature change.

M. Mohammadi [a, b *]
A. Farajpour [b]
M. Goodarzi [a]
F. Dinari [c]

[a] Department of engineering, Ahvaz branch, Islamic Azad University, Ahvaz, Iran.
[b] Department of mechanical engineering, Isfahan University of Technology, Isfahan 84156-83111, Iran.
[c] Department of physic, science faculty, Islamic azad university branch Izeh, Izeh, Iran.

*Author email: m.mohamadi@me.iut.ac.ir

1 INTRODUCTION

In the new epoch, the concentration of scientific community international has carried to the investigation of the behavior of matters at the atomic scale of material. The growth of scientists at this length scale has carried to the creating of the phrase nanotechnology. Nanotechnology is one of the most encouraging technologies to be researched now. This technology could have enormous influence on information technology, aerospace, electronic devices, defence production and medical

devices. Many endeavors have been made to construct nanodevices, expand and utilize matters on the nano scale. Some encouraging utilization has commenced to appear. One of the best examples of novel nanostructures are carbon nanotubes (CNTs). Carbon nanotubes are allotropes of carbon. These are derived by bottom-up chemical synthesis processes. In carbon nanotubes, the chemical compound and atomic bonding configuration is simple. However, these materials represent various structure-property relations among the materials. Many nanostructures based on the carbon such as CNTs (Iijima, 1991), nanorings (Kong et al., 2004), etc, are considered as deformed graphene sheet. Graphene is two-dimensional atomic crystal with excellent electronic and mechanical properties. So analysis of graphene sheets is a fundamental subject in the study of the nanomaterials. Up to this time, the mechanical behaviors of nanostructures has been studied by experimental (Ruud et al., 1994; Wong et al., 1997), continuum mechanics (Ru and Mech, 2001; Behfar and Naghdabadi, 2005) and computer simulation (Chowdhuri et al., 2010). In view of the fact that controlled experiments in nanoscale are difficult and the molecular dynamic is com- putationally expensive, the continuum mechanics has been vastly studied for mechanical proper- ties of two dimensional nanostructures. At nanometer scales, size effects often become important. The 'size-effect' is important in mechanical behaviors of materials when the size of these structures become small. This problem has been shown by experimental and atomistic simulation results. On the other hand, the use of traditional classical continuum (Yoon et al., 2003; Liew et al., 2006) models may be questionable in the analysis of nanostructures because the classical continuum elasticity cannot predict the size-effects. There are various size dependent continuum theories such as couple stress theory (Zhou and Li 2001), strain gradient elasticity theory (Akgöz and Civalek, 2011a; Akgöz and Civalek, 2012a; Akgöz and Civalek, 2013a), modified couple stress theory (Yong, 2002; Akgöz and Civalek, 2011b; Akgöz and Civalek, 2012b; Akgöz and Civalek, 2013b) and nonlocal elasticity theory (Eringen, 1983; Farajpour et al., 2011a; Danesh et al., 2012; Moha-mmadi et al., 2013a).

Ke et al. (2011) employed the modified couple stress theory for free vibration and buckling of the microbeams with the effect of the temperature change. They found that the thermal effect on the fundamental frequency and critical buckling load is slight when the thickness of the microbeam has a similar value to the material length scale parameter. Akgöz and Civalek (2012a) investigated bending analysis of micro-sized beams based on the Bernoulli-Euler beam theory. Modified strain gradient elasticity and modified couple stress theories are used in that paper. Their study highlighted that the bending values obtained by these higher-order elasticity theories have a significant difference with those calculated by the classical elasticity theory. Akgöz and Civalek (2013 b) employed modified couple stress theory for bending, buckling, and vibration of micro-sized plates on elastic medium. The surrounding elastic medium is modeled as the Winkler elastic foundation in their paper.

The nonlocal continuum theory has been usually used in the theoretical researches of structures at small scale (Reddy, 2007; Heireche et al., 2008; Wang and Duan, 2008; Aydogdu, 2009; Shen and Zhang, 2010; Wu et al., 2011; Aksencer and Aydogdu, 2011; Narendar and Gopalakrishnan, 2011; Moosavi et al., 2011; Farajpour et al., 2011b; Farajpour et al., 2012; Civalek and Akgöz, 2013; Ghorbanpour Arani et al., 2013; Mohammadi et al., 2013b) among all size-dependent theories. To overcome the disadvantages of classical elasticity theory, Eringen and Edelen (1972) introduced the nonlocal elasticity theory in 1972. He modified the classical continuum mechanics for taking into account the small scale effects. Microtubules (MTs) are important components of cytoskeletal structures, which, in conjunction with actin and intermediate filaments, provide both the static and dynamic framework that maintains cell structure. Bending, vibration and buckling analyses of microtubules have been recently investigated using the continuum model (Civalek and Demir, 2010; Civalek and Demir, 2011; Demir and Civalek, 2013). Amara et al. (2010) employed the nonlocal elasticity theory for the buckling of multiwalled carbon nanotubes (MWCNTs) under

temperature field. They reported that the thermal effect on the buckling strain is dependent on the temperature changes, the aspect ratios, and the buckling modes of carbon nanotubes. Pradhan and Phadikar (2009) investigated the vibration of embedded multilayered graphene sheets (MLGSs) based on the nonlocal elasticity theory. In their paper, they showed that the small scale effect is quite important and needs to be included in the continuum model of graphene sheet. Pradhan and Murmu (2009) investigated the buckling of single-layered graphene sheets under biaxial compression via nonlocal continuum mechanics. They reported that the nonlocal effect is quite significant in graphene sheets and has a decreasing effect on the buckling loads. When compared with uniaxially compressed graphene, the biaxially compressed one show lower influence of nonlocal effects for the case of smaller side lengths and larger nonlocal parameter values. Murmu and Pradhan (2009) studied the free in-plane vibration of nanoplates by nonlocal continuum model. They are obtained explicit relations for natural frequencies through direct separation of variables. Ansari et al. (2010) have shown that the nonlocal elasticity theory is quite accurate and reliable for the free vibration analysis of SLGSs by employing molecular dynamics modelling. Babaei and Shahidi (2010) investigated the buckling of quadrilateral nanoplates based on nonlocal elasticity theory and by using the Galerkin method. In this article, the buckling load of skew, rhombic, trapezoidal, and rectangular nanoplates considering various geometrical parameters are obtained. Pradhan and Kumar (2011) investigated vibration analysis of orthotropic graphene sheets using nonlocal elasticity theory. The solution procedure was based on the discretization of the spatial derivatives by employing the differential quadrature method (DQM) as an accurate and efficacious numerical method. In that paper, effect of boundary conditions is investigated on frequencies of vibration. With respect to developmental works on mechanical behavior analysis of SLGSs, it should be noted that none of the researches mentioned above, have considered a circular graphene sheet. Herein, Farajpour et al. (2011a) studied axisymmetric buckling of the circular graphene sheets with the nonlocal continuum plate model. In that paper, the buckling behavior of circular nanoplates under uniform radial compression is studied. Explicit expressions for the buckling loads are obtained for clamped and simply supported boundary conditions. It is shown that nonlocal effects play an important role in the buckling of circular nanoplates. In that paper, their results compared with the results obtained by molecular dynamic and it is observed that results predicted by nonlocal theory are in exactly match with Molecular dynamics (MD) results. Thus the reliability of nonlocal theory and presented solution is demonstrated. Mohammadi et al. (2013a) employed the nonlocal plate theory to analyze vibration of circular and annular graphene sheet. They found that scale effect is less prominent in lower vibration mode numbers and is highly prominent in higher mode numbers.

It is cleared that the natural frequency is easily affected by the applied in-plane pre-stressed and temperature change. As a result, the effect of in-plane pre-stressed on the property of transverse vibration of graphene sheet is of practical interest. Researches that investigated on the nonlocal circular graphene sheets are very limited in number with respect to the case of rectangular nanoplate. In the present paper, the effect of the in-plane pre-stressed and temperature change on the vibration frequency of single layered circular and annular graphene sheet is investigated. The circular and annular graphene sheet embedded in an elastic medium. The governing equation of motion is derived using the nonlocal elasticity theory. Exact solution for the frequency equations of circular and annular nanoplate with simply supported and clamped boundary conditions are derived and nonlocal parameter, in-plane pre load and temperature change appears into arguments of Bessel functions. From the results, some new and absorbing phenomena can be observed. To suitably design nano electro-mechanical system (NEMS) and micro electro-mechanical systems (MEMS) devices using graphene sheets, the present results would be useful.

2. NONLOCAL PLATE MODEL

For linear homogenous elastic body, using nonlocal continuum theory the equations of motions has the form.

$$\sigma_{ij} + f_i = \rho \ddot{u}_i \tag{1}$$

where f_i and ρ are the applied or body forces and the mass density respectively; u_i is the displacement vector; and σ_{ij} is the nonlocal elasticity stress tensor, defined by

$$\sigma_{ij}(x) = \int \lambda\left(|x-x'|,\eta\right) C_{ijkl}\varepsilon_{kl}(x')dV(x'), \ \forall x \in V, \tag{2}$$

here ε_{ij} and C_{ijkl} are the strain and fourth order elasticity tensors, respectively. $\lambda\left(|x-x'|,\eta\right)$ is the nonlocal modulus (attenuation function) incorporating into constitutive equations the nonlocal effects. $|x-x'|$ represents the distance between the two points (x and x'). η is a material constant ($\eta = e_0 l_i / a$) that depends on the internal (lattice parameter, granular size, distance between $C-C$ bonds), l_i and external characteristics lengths (crack length, wave length), l. Choice of the value of parameter e_0 is vital for the validity of nonlocal models. Hence the effects of small scale and atomic forces are considered as material parameters in the constitutive equation. This parameter was determined by matching the dispersion curves based on the atomic models. In other words, results can be justified by an approximation of the atomic dispersion relations. Eringen (1972; 1983) equated the relationship between the frequency given by Born-Karman model of lattice dynamics and that of nonlocal theory for plane waves and obtained a value of 0.39 for e_0. Wang and Wang (2007) reported that the scale factor $e_0 l_i$ of single-wall carbon nanotubes (SWCNTs) must be smaller than 2.0 nm. Therefore, in the present study the value of nonlocal parameter $e_0 l_i$ is taken in the range of 0-2 nm. The integro-partial differential equation Equation (1) based on nonlocal elasticity with that kernel function can be simplified to

$$\left(1-\left(e_0 l_i\right)^2 \nabla^2\right)\sigma^{nl} = C : \varepsilon \tag{3}$$

where ":" represents the double dot product and ∇^2 is the Laplacian operator. The nonlocal constitutive equation Equation (3) has been recently employed for the study of micro and nanostructural elements (Moosavi et al 2011; Mohammadi et al., 2013). We consider monolayer graphene sheets in our present study. In two-dimensional forms the stress–strain relations are written as;

$$\begin{Bmatrix} \sigma_{xx}^{nl} \\ \sigma_{yy}^{nl} \\ \sigma_{xy}^{nl} \end{Bmatrix} - (e_0 l_i)^2 \nabla^2 \begin{Bmatrix} \sigma_{xx}^{nl} \\ \sigma_{yy}^{nl} \\ \sigma_{xy}^{nl} \end{Bmatrix} = \begin{bmatrix} E/(1-\upsilon^2) & \upsilon E/(1-\upsilon^2) & 0 \\ \upsilon E/(1-\upsilon^2) & E/(1-\upsilon^2) & 0 \\ 0 & 0 & 2G \end{bmatrix} \begin{Bmatrix} \varepsilon_{xx} - \alpha\Delta T \\ \varepsilon_{yy} - \alpha\Delta T \\ \varepsilon_{xy} \end{Bmatrix} \tag{4}$$

where $E, G\ \upsilon$ *and* α are the Young's modulus, shear modulus Poisson's ratio and coefficient of thermal expansion, respectively. $\sigma_{xx}^{nl}, \sigma_{yy}^{nl}$ and σ_{xy}^{nl} represent the nonlocal stresses. The strains in terms of displacement components in the middle surface can be written

$$\varepsilon_{xx} = -z\frac{\partial^2 w}{\partial x^2}, \varepsilon_{yy} = -z\frac{\partial^2 w}{\partial y^2}, \varepsilon_{xy} = -\frac{\partial^2 w}{\partial x \partial y} \tag{5}$$

Stress resultants are defined as below

$$M_{xx} = \int_{-h/2}^{h/2} z\sigma_{xx}^{nl} dz, M_{yy} = \int_{-h/2}^{h/2} z\sigma_{yy}^{nl} dz, M_{xy} = \int_{-h/2}^{h/2} z\sigma_{xy}^{nl} dz \tag{6}$$

Here h denotes the thickness of the plate. By inserting Equation (4), and Equation (5) into Equation (6) we can express stress resultants in terms of lateral deflection on the classical plate theory as follows

$$\begin{gathered} M_{xx} - (e_0 l_i)^2 \nabla^2 M_{xx} = -D\left(\frac{\partial^2 w}{\partial x^2} + \upsilon \frac{\partial^2 w}{\partial y^2}\right), M_{yy} - (e_0 l_i)^2 \nabla^2 M_{yy} = -D\left(\frac{\partial^2 w}{\partial y^2} + \upsilon \frac{\partial^2 w}{\partial x^2}\right) \\ M_{xy} - (e_0 l_i)^2 \nabla^2 M_{xy} = -D(1-\upsilon)\frac{\partial^2 w}{\partial x \partial y}, \end{gathered} \tag{7}$$

Where

$$D = \frac{Eh^3}{12(1-\upsilon^2)} \tag{8}$$

Note that relations given in Equation (7) are in the nonlocal plate model and those reduce to that of the classical equation when the nonlocal parameter $e_0 l_i$ is set to zero. By using the principle of virtual work, we can obtain governing equations.

$$\begin{gathered} \frac{\partial^2 M_{xx}}{\partial x^2} + 2\frac{\partial^2 M_{xy}}{\partial x \partial y} + \frac{\partial^2 M_{yy}}{\partial y^2} + f + \frac{\partial}{\partial x}\left(N_{xx}\frac{\partial w}{\partial x} + N_{xy}\frac{\partial w}{\partial y}\right) \\ + \frac{\partial}{\partial y}\left(N_{yy}\frac{\partial w}{\partial y} + N_{xy}\frac{\partial w}{\partial x}\right) = \rho h \frac{\partial^2 w}{\partial t^2} + K_w w - K_G \nabla^2 w \end{gathered} \tag{9}$$

here f, ρ, K_w, K_G are distributed transverse load acting on the nanoplate per unit area of the nanoplate, density, Winkler modulus and the shear modulus of the surrounding elastic medium, respectively. It is assumed that the nanoplate is free from any transverse loadings $(f = 0)$ we can express stress resultants in terms of lateral deflection on the classical plate theory as follows

$$N_{xx} = N_{yy} = N_r + N_{temp}, \qquad N_{xy} = 0 \tag{10}$$

Here N_r and N_{temp} are the uniform boundary tension and resultant thermal stress respectively. On the basis of the theory of thermal elasticity mechanics, the resultant thermal stress can be written as

$$N_{temp} = \frac{E\alpha}{(1-\upsilon)} h\Delta T \tag{11}$$

So we have Using Equation (7), Equation (9) and Equation (10) we have the following governing equation of motion in terms of the displacements for the present analysis

$$\begin{gathered} D\nabla^2\left(\nabla^2 w\right) + \left(N_r + N_{temp}\right)\left(e_0 l_i\right)^2 \nabla^2\left(\nabla^2 w\right) - \rho h\left(e_0 l_i\right)^2 \nabla^2\left(\frac{\partial^2 w}{\partial t^2}\right) - \left(N_r + N_{temp}\right)\nabla^2 w \\ + \rho h \frac{\partial^2 w}{\partial t^2} + K_w w - K_G \nabla^2 w - K_w\left(e_0 l_i\right)^2 \nabla^2 w + K_G\left(e_0 l_i\right)^2 \nabla^2\left(\nabla^2 w\right) = 0 \end{gathered} \tag{12}$$

where ∇^2 is laplacian operator in polar coordinate, the two-dimensional Laplace operator is given by $\nabla^2(\ ) = \partial^2(\ )/\partial r^2 + (1/r)\partial(\ )/\partial r + (1/r^2)\partial^2(\ )/\partial\theta^2$. The parameters $D,(e_0 l_i),w$ are the flexural rigidity of the nanoplate, nonlocal parameter and transverse displacement of the circular nanoplate, respectively. For free vibration, we can write the motion of the plate in polar coordinates as

$$w(r,\theta,t) = W(r,\theta)e^{i\omega t} \tag{13}$$

where ω is the natural frequency and $i^2 = -1$. By inserting Equation (13) into Equation (12) yields a four order partial differential equation involving natural mode $W(r,\theta)$

$$\nabla^2\left(\nabla^2 W\right) + \Gamma^2\nabla^2 W - \Sigma^4 W = 0 \tag{14}$$

where,

$$\Gamma^2 = \frac{\left(\rho h\omega^2 (e_0 l_i)^2/D - \left(N_r + N_{temp}\right)/D - K_G/D - K_W(e_0 l_i)^2/D\right)}{\left(1 + \left(N_r + N_{temp}\right)(e_0 l_i)^2/D + K_G(e_0 l_i)^2/D\right)}$$
$$\Sigma^4 = \frac{\rho h\omega^2/D - K_W/D}{\left(1 + \left(N_r + N_{temp}\right)(e_0 l_i)^2/D + K_G(e_0 l_i)^2/D\right)} \tag{15}$$

Using Laplacian operator in polar coordinates, the complete solution to the above Equation (14) can be obtained by superimposing the solutions of the two following Bessel equations

$$\frac{\partial^2 W}{\partial r^2} + \frac{1}{r}\frac{\partial W}{\partial r} + \frac{1}{r^2}\frac{\partial^2 W}{\partial\theta^2} + \left(\frac{\Gamma^2 - \sqrt{\Gamma^4 + 4\Sigma^4}}{2}\right)W = 0 \tag{16}$$

$$\frac{\partial^2 W}{\partial r^2} + \frac{1}{r}\frac{\partial W}{\partial r} + \frac{1}{r^2}\frac{\partial^2 W}{\partial\theta^2} + \left(\frac{\Gamma^2 + \sqrt{\Gamma^4 + 4\Sigma^4}}{2}\right)W = 0 \tag{17}$$

We will put $W(r,\theta) = R(r)\varphi(\theta)$, in the Equations (16) and (17), afterwards these equations are written by multiplying with $r^2/\{R(r)\varphi(\theta)\}$

$$\frac{r^2}{R(r)}\left(\frac{d^2R}{dr^2} + \frac{1}{r}\frac{dR}{dr} + \left(\frac{\Gamma^2 - \sqrt{\Gamma^4 + 4\Sigma^4}}{2}\right)R(r)\right) = -\frac{1}{\varphi(\theta)}\frac{d^2\varphi(\theta)}{d\theta^2} \tag{18}$$

$$\frac{r^2}{R(r)}\left(\frac{d^2R}{dr^2} + \frac{1}{r}\frac{dR}{dr} + \left(\frac{\Gamma^2 + \sqrt{\Gamma^4 + 4\Sigma^4}}{2}\right)R(r)\right) = -\frac{1}{\varphi(\theta)}\frac{d^2\varphi(\theta)}{d\theta^2} \tag{19}$$

Equations (18) and (19) are satisfied only if each expression in the above is equal to constant ζ^2. Thus, we obtain three ordinary differential equations as

$$\frac{d^2\varphi(\theta)}{d\theta^2} + \zeta^2\varphi(\theta) = 0 \tag{20}$$

$$\frac{d^2R}{dr^2}+\frac{1}{r}\frac{dR}{dr}+\left(\frac{\Gamma^2+\sqrt{\Gamma^4+4\Sigma^4}}{2}-\frac{\zeta^2}{r^2}\right)R(r)=0 \tag{21}$$

$$\frac{d^2R}{dr^2}+\frac{1}{r}\frac{dR}{dr}+\left(\frac{\Gamma^2-\sqrt{\Gamma^4+4\Sigma^4}}{2}-\frac{\zeta^2}{r^2}\right)R(r)=0 \tag{22}$$

The solution of Equation (20) will become

$$\varphi(\theta)=A\cos(\zeta\theta)+B\sin(\zeta\theta) \tag{23}$$

Since $W(r,\theta)$ has to be a continuous function, $\varphi(\theta)$ must be a periodic function with a period of 2π so that $W(r,\theta)=W(r,\theta+2\pi)$. Thus, ζ must be an integer

$$\zeta=m \qquad m=0,1,2,... \tag{24}$$

Equation (21) is recognized as forms of Bessel's equation of order $m=\zeta$ with the argument αr whose solution is given by

$$R_1(r)=A_m^{(1)}J_m(\xi r)+A_m^{(2)}Y_m(\eta r) \tag{25}$$

J_m,Y_m are Bessel functions of order m of the first and second kind, respectively. The parameter of α in the argument of Bessel function is defined as $\xi=\sqrt{\left(\Gamma^2+\sqrt{\Gamma^4+4\Sigma^4}\right)/2}$. Equation (22) is a Bessel differential equation of order $m=\zeta$ with the argument ηr whose the solution in this case may be written as

$$R_2(r)=A_m^{(3)}I_m(\eta r)+A_m^{(4)}K_m(\eta r) \tag{26}$$

where $\eta=\sqrt{\left(-\Gamma^2+\sqrt{\Gamma^4+4\Sigma^4}\right)/2}$ and I_m,K_m are hyperbolic or modified Bessel functions of order m of the first and second kind, respectively. The general solution of Equation (12) can be expressed as

$$w(r,\theta)=\begin{pmatrix}A_m^{(1)}J_m(\xi r)+A_m^{(2)}Y_m(\xi r)\\+A_m^{(3)}I_m(\eta r)+A_m^{(4)}K_m(\eta r)\end{pmatrix}\left(A_m^*\cos(m\theta)+B_m^*\sin(m\theta)\right) \quad m=0,1,2,... \tag{27}$$

Where the constants $B_m^*,A_m^*,A_m^{(4)},A_m^{(3)},A_m^{(2)},A_m^{(1)}$ and ξ,η depend on the boundary conditions of the nanoplate.

3. IMPLEMENTATION OF BOUNDARY CONDITIONS

3.1 circular plates

3.1.1 Clamped boundary condition

Let us consider a circular nanoplate as shown in Figure 1, where a is the radius of nanoplate. Since the origin of the polar coordinate system is taken to coincide with the center of the circular plate having no internal holes or supports at the center, the terms $Y_m(\xi r)$ and $K_m(\eta r)$ must be discarded into avoid infinite deflections and stresses at $r=0$. So, for a circular nanoplate one, we take constants $A_m^{(2)},A_m^{(4)}$ as zero. Assume that the nanoplate is clamped along its contour. The boundary conditions are

$$W(a,\theta)=0 \tag{28}$$

$$\left.\frac{\partial W(r,\theta)}{\partial r}\right|_{r=a} = 0 \tag{29}$$

By inserting Equation (27) in Equation (28) and Equation (29), we have

$$A_m^{(1)} J_m(\xi a) + A_m^{(3)} I_m(\eta a) = 0 \tag{30}$$

$$A_m^{(1)} J'_m(\xi a) + A_m^{(3)} I'_m(\eta a) = 0 \tag{31}$$

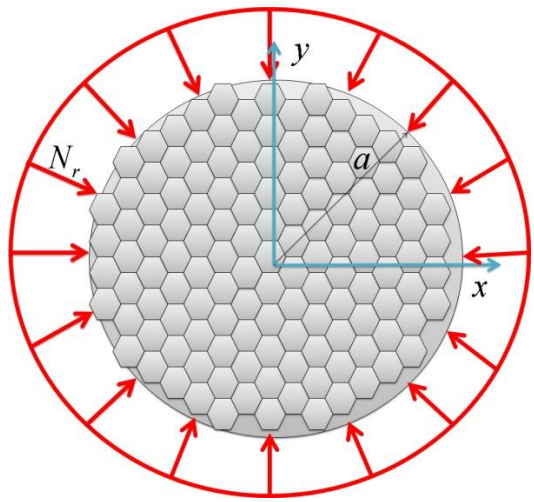

Figure 1: A continuum plate model of the circular graphene sheet

Where the primes are used to indicate a differentiation with respect to r. Using the following recursion relationships of Bessel's function

$$I'_m(\eta r) = \frac{dI_m(\eta r)}{dr} = \eta I_{m-1}(\eta r) - \frac{m}{r} I_m(\eta r) \tag{32}$$

$$J'_m(\xi r) = \frac{dJ_m(\xi r)}{dr} = \xi J_{m-1}(\xi r) - \frac{m}{r} J_m(\xi r) \tag{33}$$

Using above two equations, Equation (30) and Equation (31), are written in matrix form as

$$\begin{bmatrix} J_m(\xi a) & I_m(\eta a) \\ J'_m(\xi a) & I'_m(\eta a) \end{bmatrix} \begin{Bmatrix} A_m^{(1)} \\ A_m^{(3)} \end{Bmatrix} = 0 \tag{34}$$

This equation is satisfied in a meaningful way only if the determinant of coefficient is equal to zero. This gives the frequency equation

$$J_m(\xi a) I'_m(\eta a) - I_m(\eta a) J'_m(\xi a) = 0 \tag{35}$$

The Equation (35) can be simplified by using the Equation (32) and Equation (33)

$$\xi I_m(\eta a) J_{m-1}(\xi a) - \eta J_m(\xi a) I_{m-1}(\eta a) = 0 \tag{36}$$

where non-dimensional frequency parameter and non-dimensional preload are defined in the following form. $\Omega = \sqrt{\rho h / D}\omega a^2$, $\mathrm{N}_r^* = N_r a^2 / D$, $\mathrm{N}_{temp}^* = N_{temp} a^2 / D$, $\mu = (e_0 l_i)/a$, $\mathrm{K}_W^* = K_W a^4 / D$ $K_G^* = K_G a^2 / D$, Thus we have,

$$\xi a = \sqrt{\frac{\Gamma^2 a^2 + \sqrt{\Gamma^4 a^4 + 4\Sigma^4 a^4}}{2}} \quad \text{and} \quad \eta a = \sqrt{\frac{-\Gamma^2 a^2 + \sqrt{\Gamma^4 a^4 + 4\Sigma^4 a^4}}{2}} \tag{37}$$

$$\Gamma^2 a^2 = \frac{\Omega^2 \mu^2 - N_r^* - N_{temp}^* - K_G^* - K_W^* \mu^2}{1 + N_r^* \mu^2 + N_{temp}^* \mu^2 + K_G^* \mu^2} \quad \Sigma^4 a^4 = \frac{\Omega^2 - K_W^*}{1 + N_r^* \mu^2 + N_{temp}^* \mu^2 + K_G^* \mu^2} \tag{38}$$

3.1.2 Simply supported boundary condition

For circular nanoplate with simply supported edge, the boundary conditions are, at the boundary radius $r = a$

$$W(a,\theta) = 0 \tag{39}$$

$$\left(\frac{\partial^2 W(r,\theta)}{\partial r^2} + \frac{\upsilon}{r} \frac{\partial W(r,\theta)}{\partial r} + \frac{\upsilon}{r^2} \frac{\partial^2 W(r,\theta)}{\partial \theta^2} \right)\Bigg|_{r=a} = 0 \tag{40}$$

By inserting Equation (27) into Equation (39), Equation (40) can be written in a matrix form similar to previous section. For nontrivial solution, the characteristic determinant is set to zero. By expanding the determinant, one can get the frequency equation of circular nanoplate with simply supported boundary condition as follows

$$C_m^{(2)} J_m(\xi a) - C_m^{(1)} I_m(\eta a) = 0 \tag{41}$$

Where $C_m^{(1)}$ and $C_m^{(2)}$ are defined

$$C_m^{(1)} = J''(\xi a) + \frac{\upsilon}{a} J'(\xi a) - \frac{m^2 \upsilon}{a^2} J(\xi a) \text{ and } C_m^{(2)} = I''(\xi a) + \frac{\upsilon}{a} I'(\xi a) - \frac{m^2 \upsilon}{a^2} I(\xi a) \tag{42}$$

3.2 Annular plate

3.2.1 Clamped boundary condition in outer and inner radius

An annular plate consists of a circular outer boundary and a concentric circular inner boundary. Throughout this work the radius a and b will define the outer and inner boundaries, respectively. We consider an annular graphene sheet with clamped boundary condition on Outer and inner edges of the plate. Now, we will substitute the solution Equation (27) into the clamped boundary conditions at $r = a$ and $r = b$. So, we will have.

$$W(r,\theta)\Big|_{r=a} = W(r,\theta)\Big|_{r=b} = 0 \tag{43}$$

$$\frac{dW(r,\theta)}{dr}\Bigg|_{r=a} = \frac{dW(r,\theta)}{dr}\Bigg|_{r=b} = 0 \tag{44}$$

This will give four homogeneous equations in four unknowns $A_m^{(1)}, A_m^{(2)}, A_m^{(3)}$ and $A_m^{(4)}$. Similar to the complete circular plates in the previous section for a nontrivial solution, the determinant of coefficient will be zero. The frequency determinant will consist of Bessel function of higher orders.

$$\begin{vmatrix} J_m(\xi a) & Y_m(\xi a) & I_m(\eta a) & K_m(\eta a) \\ J'_m(\xi a) & Y'_m(\xi a) & I'_m(\eta a) & K'_m(\eta a) \\ J_m(\xi b) & Y_m(\xi b) & I_m(\eta b) & K_m(\eta b) \\ J'_m(\xi b) & Y'_m(\xi b) & I'_m(\eta b) & K'_m(\eta b) \end{vmatrix} = 0 \tag{45}$$

3.2.2 Simply supported boundary condition in outer and inner radius

For annular nanoplate with simply supported boundary conditions on outer and inner radius of the plate, the boundary conditions are defined as below:

$$W(r,\theta)\Big|_{r=a} = W(r,\theta)\Big|_{r=b} = 0 \tag{46}$$

$$\left(\frac{\partial^2 W(r,\theta)}{\partial r^2} + \frac{\upsilon}{r} \frac{\partial W(r,\theta)}{\partial r} + \frac{\upsilon}{r^2} \frac{\partial^2 W(r,\theta)}{\partial \theta^2} \right)\Bigg|_{r=a} = 0 \tag{47}$$

$$\left(\frac{\partial^2 W(r,\theta)}{\partial r^2}+\frac{\upsilon}{r}\frac{\partial W(r,\theta)}{\partial r}+\frac{\upsilon}{r^2}\frac{\partial^2 W(r,\theta)}{\partial \theta^2}\right)\Bigg|_{r=b}=0 \tag{48}$$

By inserting Equation (27) into Equations (46-48), one can write them in the matrix form (in this section the order of matrix is 4) similar to previous section. To determine nontrivial solutions of the above system of homogeneous equations, it is necessary to equate its determinant to zero. The frequency equation of annular nanoplate with simply supported boundary condition on the outer and inner radius can be written as follows:

$$\begin{vmatrix} J_m(\xi a) & Y_m(\xi a) & I_m(\eta a) & K_m(\eta a) \\ C_m^{*(J)} & C_m^{*(Y)} & C_m^{*(I)} & C_m^{*(Y)} \\ J_m(\xi b) & Y_m(\xi b) & I_m(\eta b) & K_m(\eta b) \\ C_m^{**(J)} & C_m^{**(Y)} & C_m^{**(I)} & C_m^{**(K)} \end{vmatrix}=0 \tag{49}$$

Where,

$$C_m^{*(y)}=y''(\xi a)+\frac{\upsilon}{a}y'(\xi a)-\frac{m^2\upsilon}{a^2}y(\xi a) \tag{50}$$

$$C_m^{**(y)}=y''(\xi b)+\frac{\upsilon}{b}y'(\xi b)-\frac{m^2\upsilon}{b^2}y(\xi b) \tag{51}$$

Note that the above equations are for $y=J,\ Y,\ I,\ K$. For other boundary conditions of annular nanoplate, frequency equations are derived similarly.

4 RESULTS AND DISCUSSION

Effect of thermal on the vibration of circular and annular nanoplate under in-plane pre- load investigated in this paper. We assumed that the scale coefficients are smaller than 2.0 nm because these values for CNTs were taken by Wang and Wang (2007). The properties are considered same as indicated in the reference (2006). $E=1060$ Gpa, $\upsilon=0.25$, $\rho=2250\ kg/m^3$ .For the room or low temperature case thermal coefficient is taken $\alpha=-1.6\times10^{-6}\ \mathrm{K}^{-1}$ and for high temperature case thermal coefficient is taken $\alpha=1.1\times10^{-6}\ \mathrm{K}^{-1}$. These values were used for CNTs (Zhang et al., 2007; Benzair et al., 2008; Lee et al., 2009). Single layered annular graphene sheets have been considered for the present nonlocal analyses. Following four boundary conditions have been investigated in the vibration analysis of the annular graphene sheets as:

SS: Annular graphene sheet with simply supported outer and inner radius.
CS: Annular graphene sheet with clamped outer and simply supported inner radius.
SC: Annular graphene sheet with simply supported outer and clamped inner radius.
CC: Annular graphene sheet with clamped outer and inner radius.

The non-dimensional natural frequency becomes equal zero when the in-plane compressive pre-stressed achieve their critical value and the mode of vibration is buckled. We compared the results of circular nanoplates with published data. As shown in Figure 2 results of Farajpour et al. (2011), compared to results obtained by present work for the critical compressive pre-stressed of circular nanoplates without thermal change and elastic medium. Axisymmetric problem $(m=0)$, here, is considered and nonlocal parameter of circular nanoplate is given 1nm. It can be observed that represented results exactly match with other results reported.

For further validations, present results are compared to that obtained based on nonlocal elasticity theory for square nanoplate (Pradhan and Phadikar, 2009) solutions without in-plane pre-stressed, thermal change and elastic medium. The natural frequency parameters of circular and

square nanoplate for simply support boundary conditions were presented in Table 1. Given values of radius of circular nanoplate $a=10$ nm and length of square nanoplate $L=20$ nm have been used in this analysis. The non-dimensional natural frequency in Table 1 is defined as $\overline{\Omega}=\omega\times L^2\times\sqrt{\rho h/D}/\pi^2$ where L is explained $L=2a$ for circular nanoplate and L as defined length of square for square nanoplate.

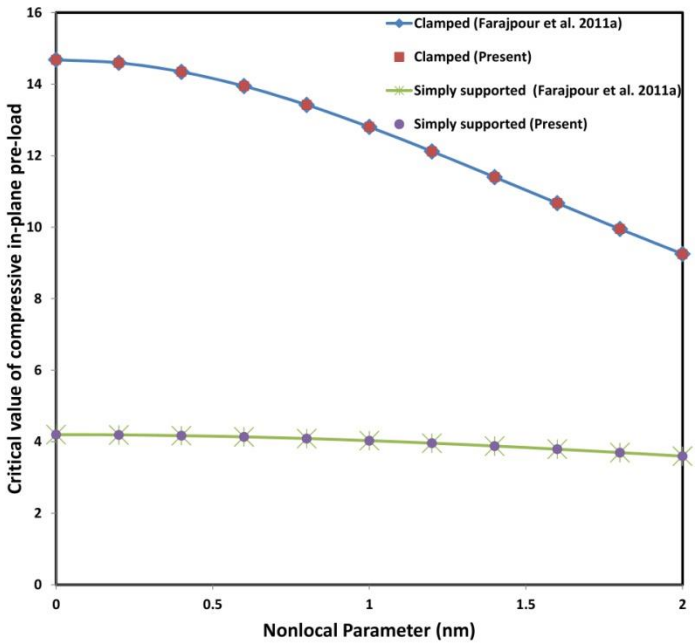

Figure 2: Comparison of results of critical value of compressive in-plane pre-stressed obtained by the present study and that obtained by Ref. (Farajpour et al. 2011a)

Results	e_0l_i (nm)										
	0	0.2	0.4	0.6	0.8	1	1.2	1.4	1.6	1.8	2
Pradhan and Phadikar 2009	2.000	1.998	1.992	1.982	1.969	1.952	1.932	1.909	1.884	1.857	1.827
Mohammadi et al. 2013a	2.000	1.997	1.990	1.974	1.964	1.944	1.921	1.895	1.866	1.835	1.802
Present	2.000	1.997	1.990	1.974	1.964	1.944	1.921	1.895	1.866	1.835	1.802

Table 1: Comparison of non-dimensional fundamental natural frequency of square nanoplate with circular one (simply support boundary condition).

Figure 3 shows the frequency difference percent with respect to nonlocal parameter. It is seen that the frequency difference percent increases with the increase of the temperature change. Also, the results show that the difference percent increases monotonically by increasing the nonlocal parameter. In other words, that nonlocal solution for difference percent is larger than the local solutions. In Figs. 3, the gap between low and high temperature cases increases with increasing the temperature change.

The relationships between non-dimensional frequency versus temperature change for different boundary condition and low and high temperature case are demonstrated in Figure 4. From Figure 4 it is observed that the non-dimensional frequency of the low temperature case is always larger than that of high temperature case. It is demonstrated that the non-dimensional frequency decreases as the change in temperature increases at higher temperature but increases as the change in temperature increases at room or low temperature. Furthermore, the gaps between the

two curves (high and low) increases with increasing the temperature change. In other words, the difference between the non-dimensional natural frequencies calculated by high temperature and low temperature decreases with decreasing temperature change. The temperature change is important for graphene sheet with simply supported boundary condition because the slope of curve with simply supported boundary conditions is more than clamped boundary condition curves.

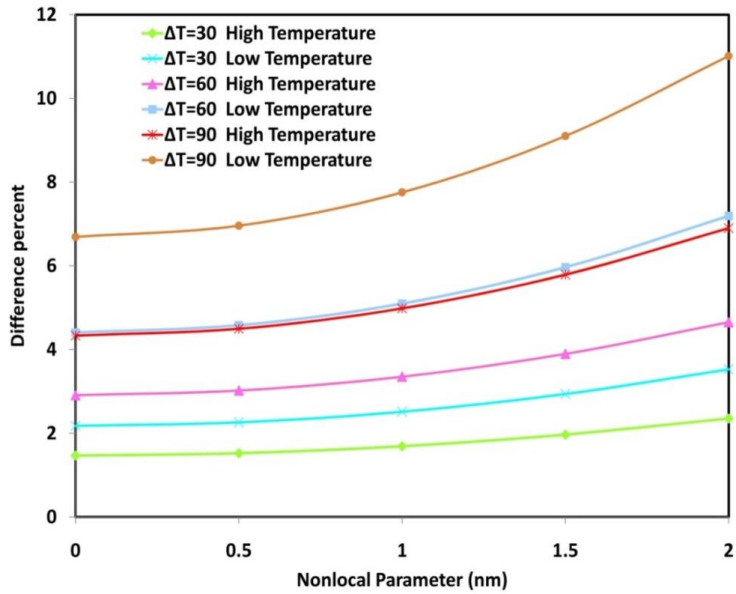

Figure 3: Variation of difference percent with nonlocal parameter for the cases low and high temperature and various changes temperature.

To study the influence of temperature change on difZference percent of non-dimensional frequency of nanoplate, the results from the solution for nondimensional frequency of nanoplate for simply supported boundary condition and for different temperature change, are plotted in Figure 5. The nonlocal parameter is taken 1 nm and high temperature case is considered in this figure. Figure 5 shows the difference percent versus radius of circular nanoplate. It is cleared that the difference percent increase with increase in temperature. It is demonstrated that as the radius of circle increases the difference percent also increases. In other words, at larger radius of circular nanoplate, the effect of temperature change is more importance.

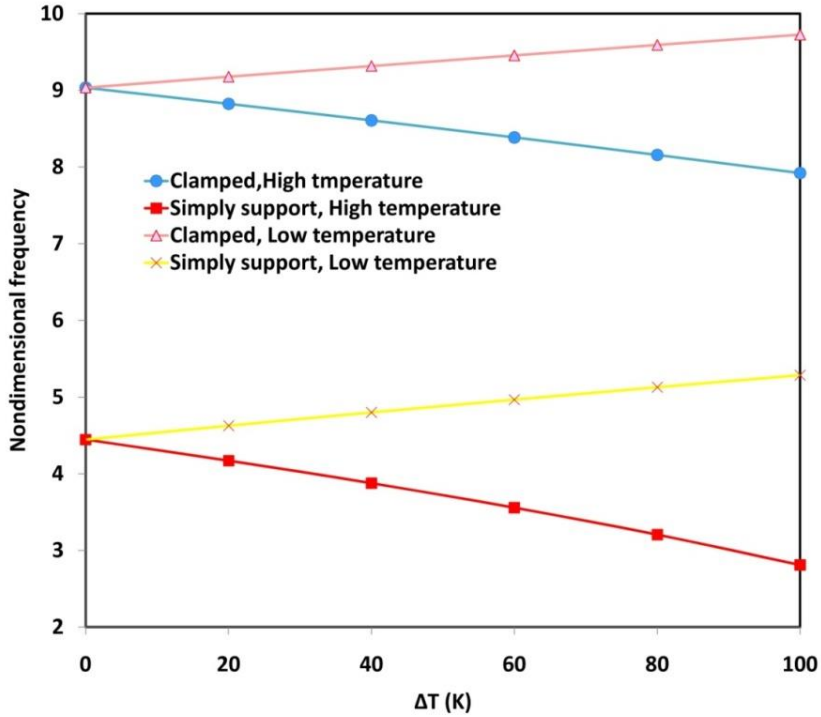

Figure 4: Change non-dimensional frequency with temperature change for various boundary conditions in the case of low and high temperature.

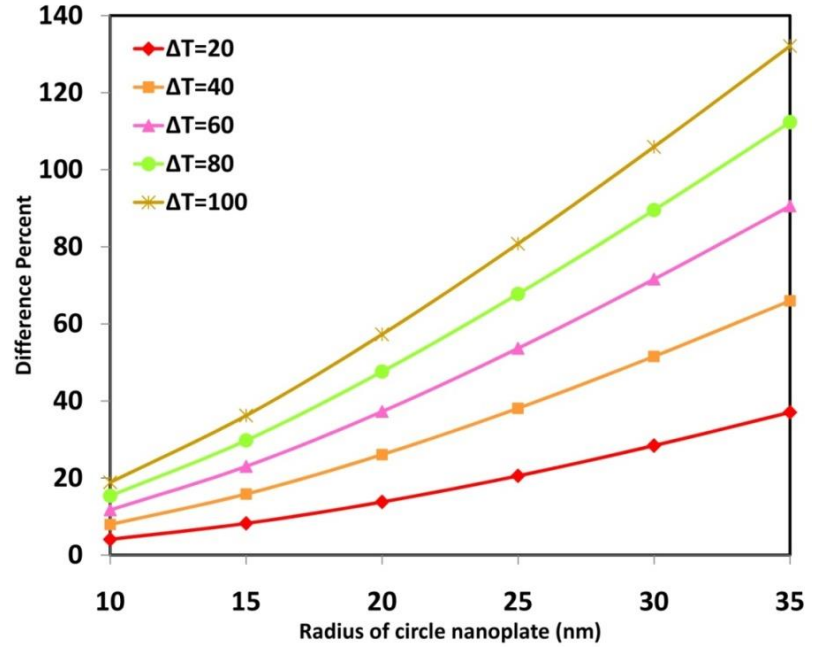

Figure 5: Change difference percent with radius of circle for various temperature changes.

Table 2 presents the change of the frequency parameters with temperature change for the annular nanoplates with $\upsilon = 0.3$. To illustrate the effect of boundary condition and thermal case on frequency response, in this section we tabulate the lowest six temperature change for different thermal case and four cases different boundary conditions of annular nanoplate. In this investigation, we consider the non-dimensional frequency of first mode number, the outer radius of the annular

nanoplate 20 nm and the nonlocal parameter is 1 nm. From this table it is seen that frequency parameters increase with increase of temperature change for all boundary condition and room or low temperature case. In the other hand, it is observed that the effects of the temperature change on the non-dimensional frequency are different for the case of low and high temperature. From this table obvious the important influence of temperature change, in the cases low and high temperature case on the non-dimensional frequency of annular graphene sheet.

Boundary Condition	Thermal Case	Temperature Change					
		0	20	40	60	80	100
CC	room or low temperature case	76.5525	77.8325	79.1066	80.3738	81.6336	82.8852
	high temperature case	76.5525	75.6695	74.7852	73.8997	73.0137	72.1283
SS	room or low temperature case	35.9875	37.7473	39.2251	40.4844	41.5775	42.5442
	high temperature case	35.9875	34.5823	33.0095	31.2912	29.4905	27.7019
CS	room or low temperature case	53.7851	55.5609	57.34	59.115	60.8793	62.6257
	high temperature case	53.7851	52.5694	51.3603	50.1594	48.9681	47.7875
SC	room or low temperature case	57.814	58.233	58.678	59.1565	59.6778	60.2523
	high temperature case	57.814	57.5377	57.2685	57.006	56.7471	56.4914

Table 2: Change of dimensionless frequency parameters for the four cases different boundary conditions and different temperature change. $\left(\Omega = \omega a^2\sqrt{\rho h/D},\ a = 20\ nm,\ b/a = 0.5\ \mathrm{e}_0 l_i = 1\ \mathrm{nm}\right)$

To illustrate the effect of aspect ratio on the non-dimensional frequency, in this section, the non-dimensional frequency versus temperature change of annular nanoplate for different aspect ratio is plotted in Figure 6. Figure 6 shows the important influence of aspect ratio on the natural frequency of annular graphene sheet with CC boundary conditions and low temperature case. The radius of circular nanoplate a=10 nm and nonlocal parameter $\mathrm{e_o l_i}$=1 nm are considered. It is found that the non-dimensional frequency increases with increase of aspect ratio from 0.1 to 0.5 and temperature change in low temperature case. Similarly these phenomena are observed for annular nanoplate with different boundary conditions. The effect of temperature change on the frequency of circular graphene sheet embedded in an elastic medium is studied. The Winkler modulus parameter $\mathrm{K_W}$, for the surrounding polymer matrix is gotten in the range of 0–400. Then shear modulus factor $\mathrm{K_G}$ is gotten in the range 0-10. Similar values of modulus parameter were also applied by Liew et al. (2006). The relationships between frequency difference percent versus Winkler constant K_W and shear modulus K_G for different temperature changes and low and high temperature case are demonstrated in Figure 7a, b. A scale coefficient $\mathrm{e_0 l_i}$ = 2.0 nm is used in the analysis. As can be seen, the Winkler constant or shear modulus decreases then the effect of thermal on the difference percent increases. It can be seen for the results that the difference percent increases with increasing the temperature change. For larger temperature change, the decline of difference percent is quite important. Also, the difference percent for low temperature case is larger than that for case of high temperature.

Furthermore the decline for the high temperature case is much less than that for case of low temperature. From these plots obvious the important influence of temperature change, in the cases low and high temperature case on the non-dimensional frequency of embedded orthotropic graphene sheet. In Figs. 7a, b the gap between low and high temperature cases increases with increasing the temperature change.

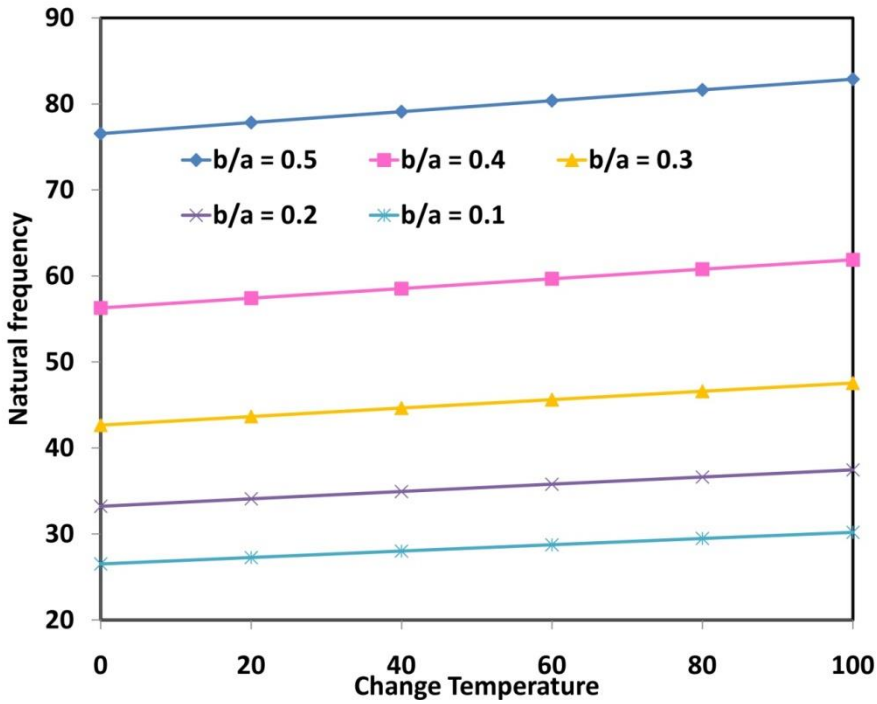

Fig 6: Change non-dimensional natural frequency with change temperature for various aspect ratios.

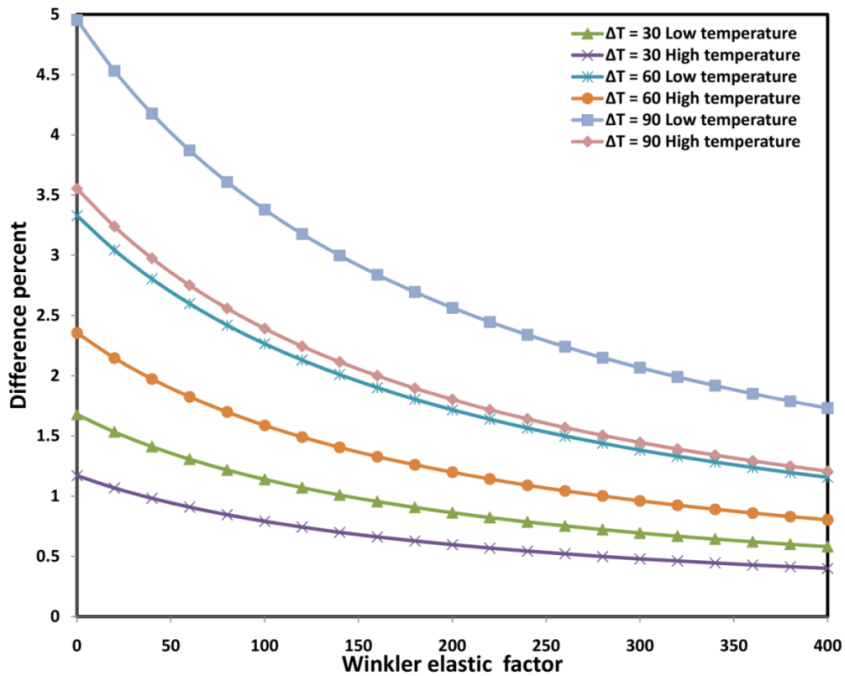

(a)

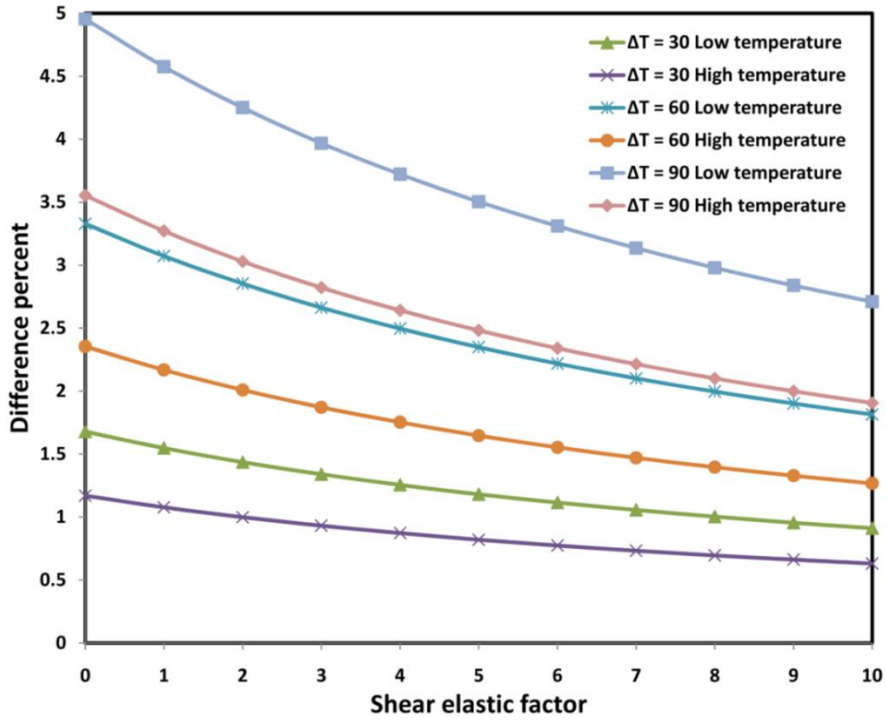

(b)

Figure 7: Change difference percent frequency of circular nanoplate versus a) Winkler elastic factor, b) shear elastic factor, for low and high temperature case and various temperature changes.

Variation of frequencies with Winkler elastic factor is shown for first mode of annular nanoplate with CC boundary condition in Figure 8. The frequencies are computed considering radius of circular nanoplate r=10 nm. The frequency curves show that the non-dimensional frequencies are sensitive to the elastic medium. As the Winkler modulus parameter increases the non-dimensional frequency also increase. This increasing trend of non-dimensional frequency parameter with surrounding matrix is noticed to be influenced significantly by temperature change. This interprets that if the circular graphene sheets are embedded in a soft elastic medium, fundamental frequency will be quite low for very small size circular graphene sheet as depicted in this figure. For lower values of e0a the non-dimensional natural frequency are higher while this is lower for large e0a values. This interprets that if the circular graphene sheets are embedded in a soft elastic medium, the nondimensional natural frequency will be quite low. The difference between two curves increases with by increase mode number. It is seen that effect of small length scale is higher for higher wave modes. This can be clearly seen from Figure 8.

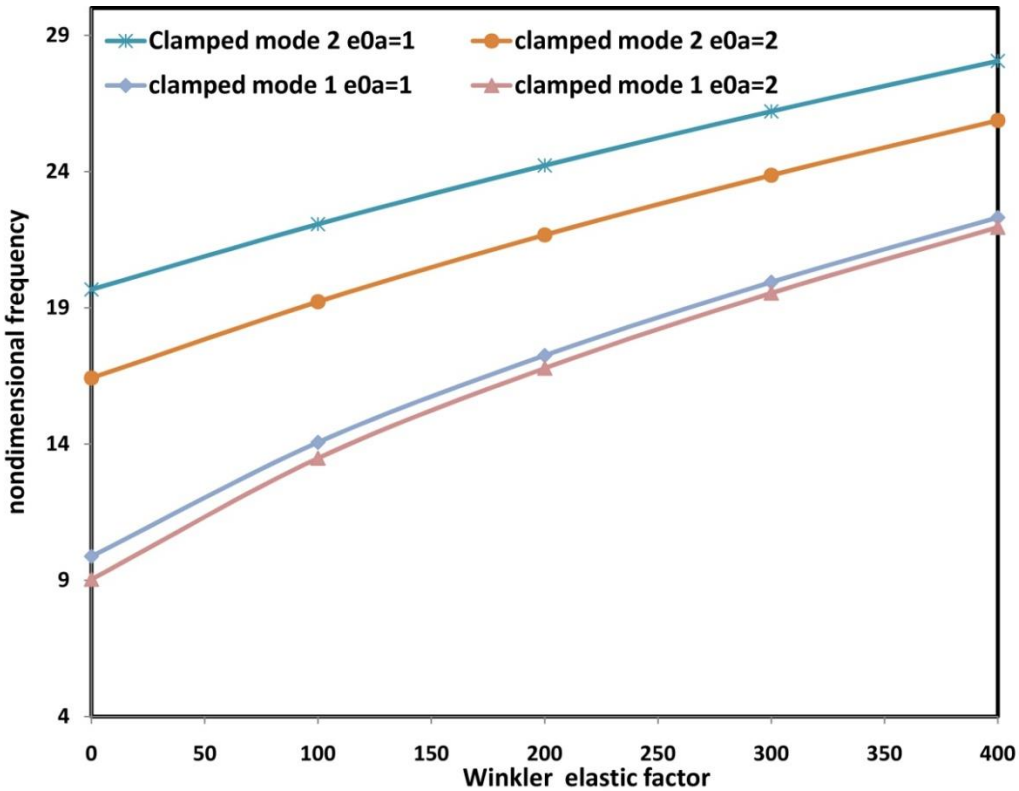

Figure 8: Change non-dimensional frequency of circular nanoplate versus Winkler elastic factor for clamp and simply boundary condition and various nonlocal parameters.

Figure 9 shows the important influence of elastic medium. The radius of circular nanoplate r=10 nm and Winkler elastic factor K_W=400 are considered. It is found that the nondimensional frequency increases with increase of shear modulus factor from 0 to 10. As can be observed, the effect of nonlocal parameter on the non-dimensional natural frequency is less importance for circular graphene sheet embedded in an elastic medium in comparison with circular graphene sheet without elastic medium because the shear modulus increases then the effect of nonlocal parameter on the nondimensional frequency decreases. Similarly these phenomena are observed for annular nanoplate with different boundary conditions.

In Figure 10 and 11, we consider a mono-layered circular graphene sheet with clamp boundary conditions. To illustrated the influence in-plane pre-stressed on the natural frequency in two cases compressive and tensile pre-stressed, we define frequency fraction as divide non-dimensional natural frequencies with the in-plane pre-stressed by those without the in-plane pre-stressed as the following form:

$$\text{frequency fraction} = \frac{\text{Nondimensional frequency with the inplane pre} - \text{load}}{\text{Nondimensional frequency without the inplane pre} - \text{load}}$$

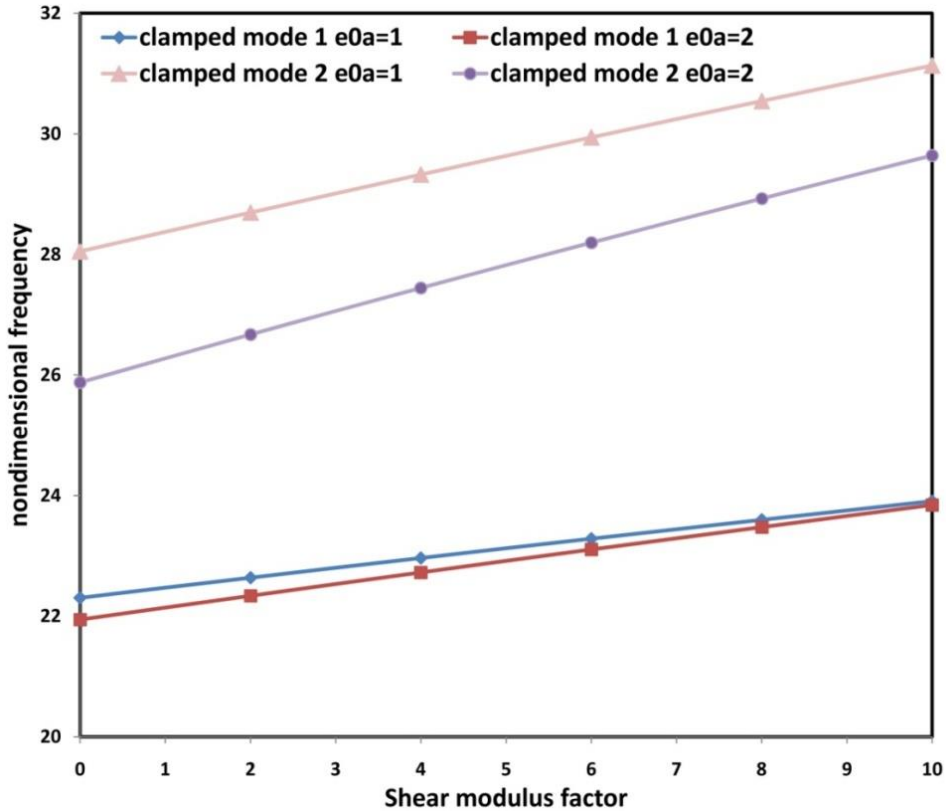

Figure 9: Change non-dimensional frequency of circular nanoplate versus shear elastic factor, for clamp and simply boundary condition and various nonlocal parameters.

The scale coefficient is 2 nm and the first mode number is considered. The in-plane loads are considered P_0=2, 4, 6, 8 and 10 for tensile pre-stressed case and P_0=1, 2, 3and 4 for compressive pre-stressed. In Figure 10 frequency fraction is plotted versus radius of circular nanoplate for various compressive in-plane pre-stressed. It is shown that the frequency fraction with different in-plane compressive loads will increase with the radius of nanoplate increasing. However, it is cleared the non-dimensional frequency with in-plane compressive loads are smaller than the non-dimensional frequency without in-plane loads for all radius of circular nanoplate. It can also be observed that the frequency fraction will increases with the in-plane load decreasing. The plot of frequency fraction with respect to radius of circular nanoplate for the case of tensile in-plane pre-stressed is demonstrated in Figure 11. It is cleared; the behaviors of the frequency fractions for the tensile in-plane pre-stressed are against compressive in-plane pre-stressed in Figure 11. In the two case of in-plane pre-stressed (compressive and tensile loads), the effect of in-plane pre-stressed decreases with the increasing of radius of circular nanoplate. This means that at larger radius of circular nanoplate, the effect of in-plane pre-stressed is less importance.

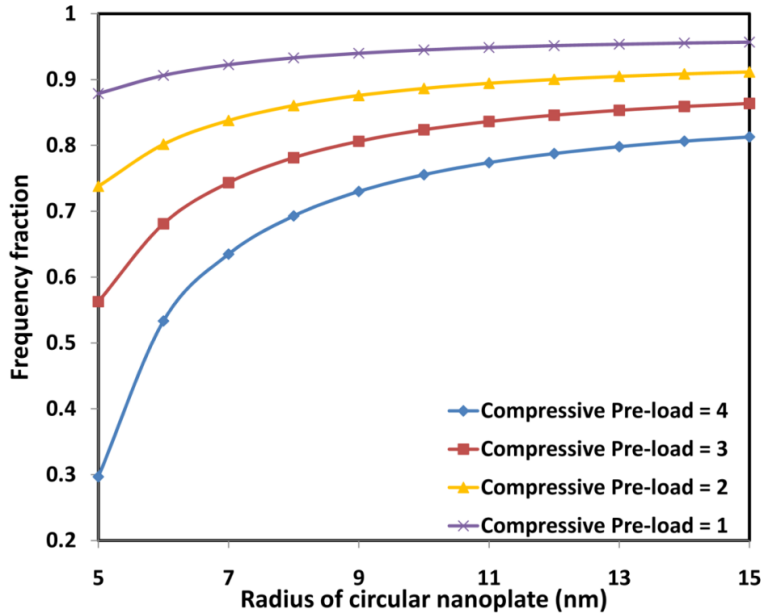

Figure 10: Change of frequency fraction with radius of circular nanoplate for various non-dimensional compressive pre-stressed.

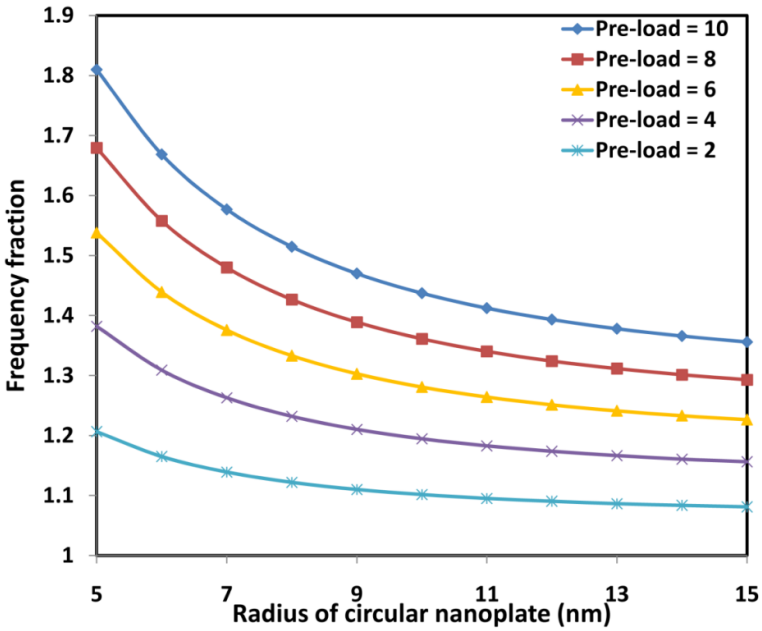

Figure 11: Change of frequency fraction with radius of circular nanoplate for various non-dimensional tensile pre-stressed.

In Figure 12, the plot of non-dimensional natural frequency with respect to radius of circular nanoplate is demonstrated. These results are plotted here for the circular nanoplate under compressive pre-stressed, the case of circular nanoplate without in-plane pre-stressed and different values of nonlocal parameter. The clamped boundary condition and first mode number is considered. From Figure 12 it is observed that decreasing the nonlocal parameter yields to increases the natural frequency. This indicates that increasing the nonlocal parameter leads to decrease in the stiffness of body. Furthermore, the non-dimensional natural frequency increases the radius of the na-

noplate increases. It is clear as a matter of fact that, the influence of nonlocal effect reduces, by increasing of radius. Furthermore, with further increase of radius the curves become smooth in nature. Nearly, at $a \geq 50$ nm all results close to the classical frequencies$\left(e_0 l_i = 0\right)$, this insinuates that the nonlocal effect decreases with growth of the plate radius and disappears after a certain radius. This may be explained that the wave length gets larger by decreasing of radius which increases the effect of the small radius scale. Moreover, the non-dimensional natural frequency for circular nanoplate with in-plane pre-stressed is smaller than that without in-plane pre-stressed. The influence of nonlocal parameter is larger for circular nanoplate with in-plane pre-stressed in comparison with circular nanoplate without in-plane pre-stressed. Further, at circular nanoplate with in-plane pre-stressed all results converge to the local frequency $\left(e_0 l_i = 0\right)$ at higher radiuses. It is seen that influence of nonlocal effect is higher for circular nanoplate with in-plane pre-stressed.

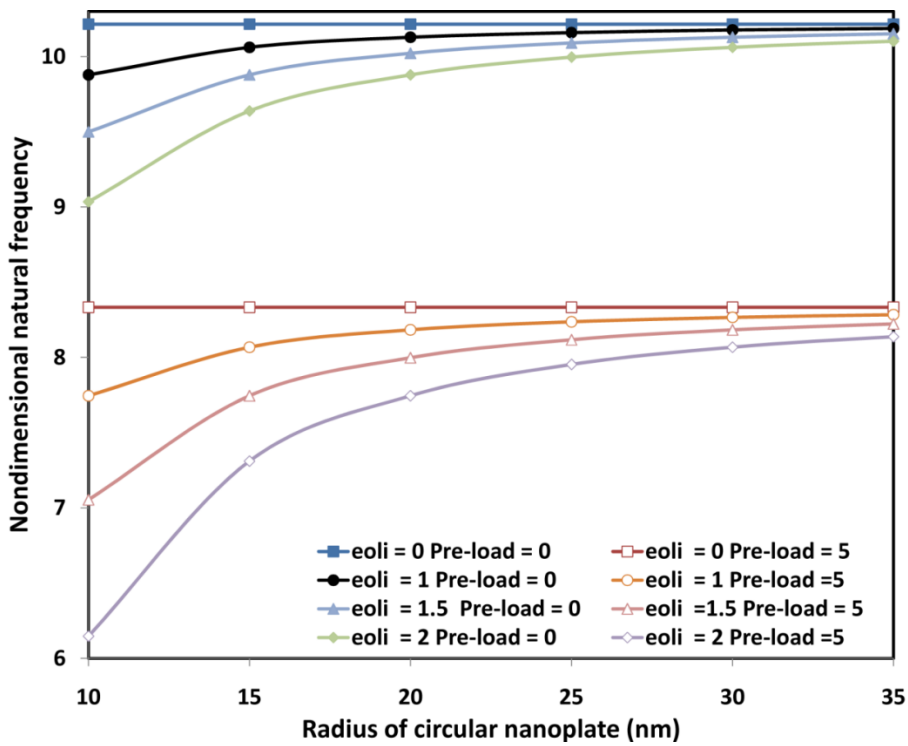

Figure 12: Variation of non-dimensional frequency with radius of a circular graphene sheet for various nonlocal parameters with in-plane pre-stressed and without in-plane pre-stressed.

Figures 13 and 14 present the comparison of the lowest five frequency parameters for the annular nanoplates with outer radius 20 nm, aspect ratio 0.5 and SS boundary condition. To illustrate the effect of nonlocal parameter and temperature change on the mode numbers, in this section we plot the lowest five frequency parameters for different nonlocal parameters and low temperature case. From this Figures it is seen that frequency parameters increase with decrease of nonlocal parameter and those increase with increasing temperature change for all mode numbers in low temperature case. However, small scale effects are more important in higher mode numbers. As seen from these Figures, the small scale effect also depends on the temperature change. The effect of nonlocal parameter on the frequency of vibration without temperature change compare to the frequency with temperature change is more important. As the temperature change increases, the small scale effect kept on decreasing. The small scale effect for vibration with thermal case is

much less than that for vibration without thermal case. Therefore, in the vibration analyses it is needful to include the nonlocal elasticity theory for higher mode number and lower temperature change.

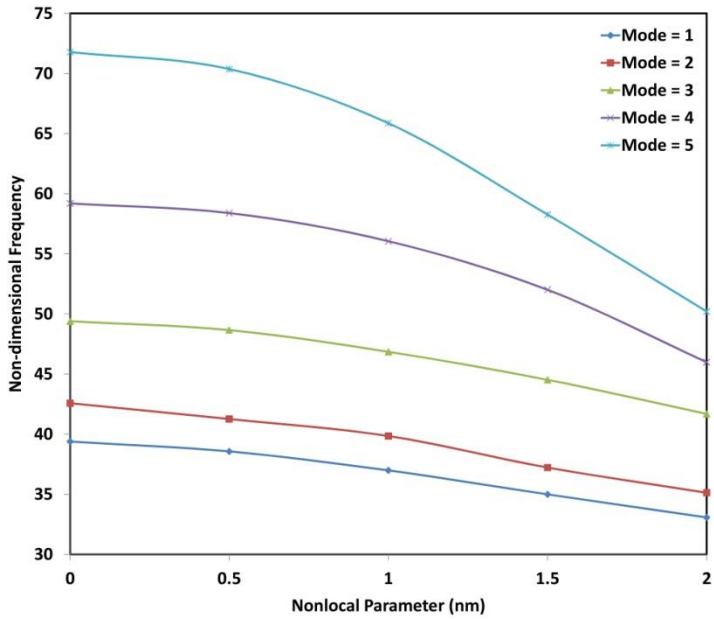

Figure 13: Variation of non-dimensional frequency of annular nanoplate with Nonlocal parameter for various mode numbers, ΔT=0 K.

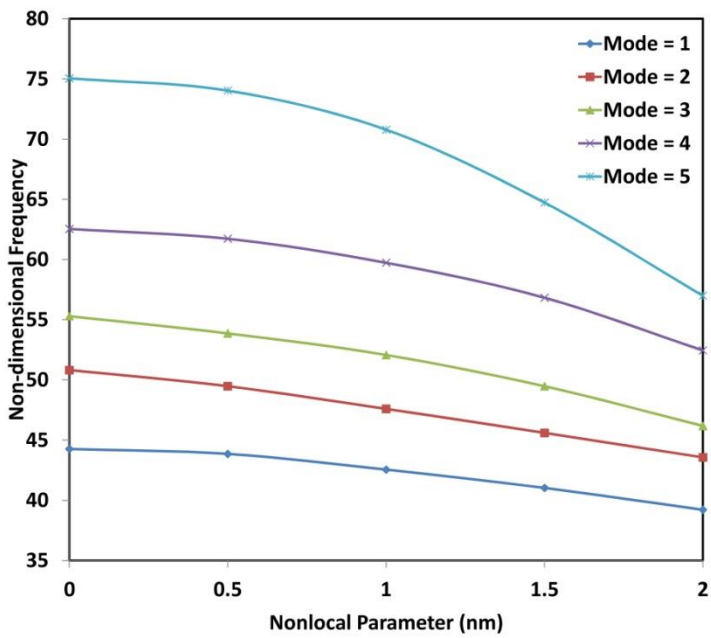

Figure 14: Variation of non-dimensional frequency of annular nanoplate with Nonlocal parameter for various modes numbers, ΔT=100 K.

The non-dimension frequency against the Winkler and Pasternak modulus (K_W and K_G) for different values of the nonlocal parameter and temperature change is tabulated in Table 3. The radius of the circular grapheme sheet is taken as 20 nm. The value of nonlocal parameter is taken in

the range of 0–2 nm. Computation has been carried out considering temperature change in the range of 0–100 K at room temperature. As the Winkler and Pasternak coefficients increase, the non-dimension frequency increases for all values of the nonlocal parameters. This is due to the fact that increasing Winkler and Pasternak coefficients increase the sheet stiffness. The effect of nonlocal parameter decreases for higher values of the Winkler and Pasternak modulus. Furthermore, the amounts of non-dimensional frequency decrease by increasing the nonlocal parameter. This implies that the stiffness of structure decreases with an increase in the nonlocal parameter for a fixed value of temperature change. It is also observed that non-dimensional frequency increases as the value of temperature change increases from 0 to 100 K. In room or low temperature case, the small scale effects are more noticeable for the single-layered graphene sheets (SLGSs) without thermal effect compared to SLGSs with positive temperature change and size effect decreases with increase in the temperature change. This means that nonlocal effects decrease with the increase of temperature change. When the environment temperature increases, the average distance between atoms increases (the interaction between atoms decreases) and it causes a decrease in the small scale effects.

Elastic medium		$e_0 l_i$ (nm)					
		ΔT=0 K			ΔT=100 K		
		0	1	2	0	1	2
K_W=0	K_G=0	10.2158	10.1284	9.8789	12.7891	12.7694	12.7129
K_W=200	K_G=0	17.446	17.395	17.2508	19.0673	19.0541	19.0162
	K_G=10	19.3082	19.3005	19.2782	20.7567	20.7828	20.8534
K_W=400	K_G=0	22.4580	22.4184	22.3068	23.7395	23.7288	23.6985
	K_G=10	23.9334	23.9272	23.9092	25.1166	25.1381	25.1965

Table 3: Change of dimensionless frequency parameters for different elastic medium, nonlocal parameter and different temperature change. $\left(\Omega = \omega a^2 \sqrt{\rho h / D},\ a = 20\ nm\right)$

5 CONCLUSIONS

This study illustrates the significance of small scale effects and temperature change on the vibration behavior of SLGSs under in-plane pre-stressed via nonlocal continuum mechanics. The closed form solutions for the free vibration nanoscale circular and annular nanoplates are obtained. Results for circular and annular graphene sheets with simply supported, clamped and mix of them are presented. From the results following conclusions are noticeable:

- By increasing in-plane tensile pre-stress the natural frequencies increases and the higher in-plane compressive pre-stress leads to lower natural frequencies.
- In the case of compressive in-plane pre-stressed the frequency fraction will increase with the radius of nanoplate increasing and in-plane pre-stressed.
- At smaller radius of circular nanoplate, the effect of in-plane pre-stressed is more importance.
- The influence of nonlocal effect reduces, by increasing of radius.
- The influence of nonlocal effect is higher for circular nanoplate with in-plane pre-stressed.
- The non-dimensional natural frequency decreases at high temperature case with increasing the temperature change.
- The effect of temperature change on the non-dimensional frequency vibration becomes the opposite at low temperature case in compression with the high temperature case.

- The nonlocal effect also depends on the temperature change. The influence of nonlocal effect for higher temperature case is much more than that for room temperature case.
- The difference percent increases monotonically by increasing the nonlocal parameter.
- The difference between low and high temperature cases increases with increasing the temperature change.
- The effect of thermal on the frequency vibration increases with increasing the radius of circular nanoplate.
- The sheet stiffness increases with increasing the Winkler and Pasternak coefficients.
- The effect of nonlocal parameter decreases for higher values of the Winkler and Pasternak modulus.
- The effects of small length scale and surrounding elastic medium are significant to the mechanical behavior of nanoplates or SLGSs and cannot be ignored.
- When the environment temperature increases, the average distance between atoms increases (the interaction between atoms decreases) and it causes a decrease in the small scale effects.

References

Akgöz B., Civalek Ö. (2011a).Application of strain gradient elasticity theory for buckling analysis of protein microtubules. Current Applied Physics 11: 1133-1138.

Akgöz B., Civalek Ö. (2011b). Strain gradiant and modified couple stress models for buckling analysis of axially loaded micro-scales beam. International Journal of Engineering Science 49: 1268-1280.

Akgöz B., Civalek Ö. (2012a).Analysis of micro-sized beams for various boundary conditions based on the strain gradient elasticity theory. Archive of Applied Mechanics 82: 423-443.

Akgöz B., Civalek Ö. (2012b). Free vibration analysis for single-layered graphene sheets in an elastic matrix via modified couple stress theory. Materials & Design 42: 164-171.

Akgöz B., Civalek Ö. (2013a). A size-dependent shear deformation beam model based on the strain gradient elasticity theory. International Journal of Engineering Science 70: 1-14.

Akgöz B., Civalek Ö. (2013b). Modeling and analysis of micro-sized plates resting on elastic medium using the modified couple stress theory. Meccanica 48: 863-873.

Aksencer T., Aydogdu M. (2011). Levy type solution method for vibration and buckling of nanoplates using nonlocal elasticity theory. Physica E 43: 954-959.

Amara K., Tounsi A., Mechab I., Adda Bedia E. A. (2010). Nonlocal elasticity effect on column buckling of multiwalled carbon nanotubes under temperature field. Applied Mathematical Modelling 34: 3933–3942.

Ansari R., Sahmani S., Arash B. (2010). Nonlocal plate model for free vibrations of single-layered graphene sheets. Physics Letters A 375: 53-62.

Aydogdu M. (2009). Axial vibration of the nanorods with nonlocal continuum rod model. Physica E 41: 861-864.

Babaei H., Shahidi A. R. (2010). Small-scale effects on the buckling of quadrilateral nanoplates based on nonlocal elasticity theory using the Galerkin method. Archive Applied Mechanic 81: 1051–1062.

Behfar K., Naghdabadi R. (2005). Nanoscale vibrational analysis of a multi-layered graphene sheet embedded in an elastic medium. Composite Science Technology 65: 1159–1164.

Benzair A., Tounsi A., Besseghier A., Heireche H., Moulay N., Boumia L. (2008). The thermal effect on vibration of single-walled carbon nanotubes using nonlocal Timoshenko beam theory. Journal of Physics D: Applied Physics 41: 225404.

Chowdhury R., Adhikari S., Wang C.W., Scarpa F. (2010). A molecular mechanics approach for the vibration of single walled carbon nanotubes. Computational Material Science 48: 730–735.

Civalek Ö., Akgöz B. (2013). Vibration analysis of micro-scaled sector shaped graphene surrounded by an elastic matrix. Computational Materials Science 77: 295-303.

Civalek Ö., Demir C., Akgöz B. (2010). Free Vibration and Bending Analyses of Cantilever Microtubules Based On Nonlocal Continuum Model. Mathematical and Computational Applications 15: 289-298.

Civalek Ö., Demir Ç. (2011).Bending analysis of microtubules using nonlocal Euler-Bernoulli beam theory.

Applied Mathematical Modeling 35:2053-2067.

Demir Ç., Civalek Ö. (2013). Torsional and Longitudinal Frequency and Wave Response of Microtubules based on the Nonlocal Continuum and Nonlocal Discrete Models. Applied Mathematical Modeling http://dx.doi.org/10.1016/j.apm.2013.04.050067.

Danesh M., Farajpour A., Mohammadi M., (2012). Axial vibration analysis of a tapered nanorod based on nonlocal elasticity theory and differential quadrature method. Mechanics Research Communications 39: 23–27.

Eringen A.C. (1983). On differential equations of nonlocal elasticity and solutions of screw dislocation and surface waves. Journal of Applied Physics 54: 4703-4711.

Eringen A.C., Edelen D.G.B. (1972). On nonlocal elasticity. International Journal Engineering Science 10: 233–48.

Farajpour A., Mohammadi M., Shahidi A.R., Mahzoon M. (2011a). Axisymmetric buckling of the circular graphene sheets with the nonlocal continuum plate model. Physica E 43: 1820 –1825.

Farajpour A., Danesh M., Mohammadi M., (2011b).Buckling analysis of variable thickness nanoplates using nonlocal continuum mechanics. Physica E 44: 719 –727.

Farajpour A., Danesh M., Mohammadi M., (2012).Buckling of orthotropic micro/nanoscale plates under linearly varying in-plane load via nonlocal continuum mechanics. Composite Structures 94: 1605–1615.

Ghorbanpour Arani A., Kolahchi R., Vossough H. (2012). Nonlocal wave propagation in an embedded DWBNNT conveying fluid via strain gradient . Physica B: Condensed Matter 407: 4281 – 4286.

Heireche H., Tounsi A., Benzair A., Maachou M., Adda Bedia E.A. (2008). Sound wave propagation in single-walled carbon nanotubes using nonlocal elasticity. Physica E 40: 2791–2799.

Iijima S. (1991). Helical microtubules of graphitic carbon. Nature 354: 56–58.

Ke, L.-L.,Wang, Y.-S., Wang Z.-D. (2011). Thermal effect on free vibration and buckling of size-dependent microbeams. Physica E 43, 1387-1393.

Kong X.Y., Ding Y., Yang R., Wang Z.L. (2004). Single-Crystal Nanorings Formed by Epitaxial Self-Coiling of Polar Nanobelts. Science 303: 1348-1351.

Lee H.L., Chang W.J. (2009). A Closed-Form Solution for Critical Buckling Temperature of a Single-Walled Carbon Nanotube. Physica E 41: 1492–4.

Liew K.M., He X.Q., Kitipornchai S. (2006). Predicting nanovibration of multi-layered graphene sheets embedded in an elastic matrix. Acta Material 54: 4229–4236.

Mohammadi M., Ghayour M., Farajpour A. (2013a). Free transverse vibration analysis of circular and annular graphene sheets with various boundary conditions using the nonlocal continuum plate model. Composites Part B 45: 32-42.

Mohammadi M., Goodarzi M., Ghayour M., Farajpour A. (2013b). Influence of in-plane pre-load on the vibration frequency of circular graphene sheet via nonlocal continuum theory. Composites Part B 51: 121-129.

Moosavi H., Mohammadi M., Farajpour A., Shahidi S. H. (2011). Vibration analysis of nanorings using nonlocal continuum mechanics and shear deformable ring theory. Physica E 43: 1820 –1825.

Murmu T., Pradhan S. C. (2009). Small-scale effect on the free in-plane vibration of nanop lates by nonlocal continuum model. Physica E 41: 1628 –1633.

Narendar S., Gopalakrishnan S. (2011). Axial wave propagation in coupled nanorod system with nonlocal small scale effects. Composites: Part B 42: 2013–23.

Pradhan S.C., Phadikar J.K. (2009). Small scale effect on vibration of embedded multi layered graphene sheets based on nonlocal continuum models. Physics Letters A 373: 1062–1069.

Pradhan S.C., Murmu T. (2009). Small scale effect on the buckling of single-layered graphene sheets under biaxial compression via nonlocal continuum mechanics. Computational Materials Science 47: 268–274.

Pradhan S.C., Kumar A. (2011). Vibration analysis of orthotropic graphene sheets using nonlocal elasticity theory and differential quadrature method. Composite Structures 93: 774–779.

Pradhan S.C., Phadikar J.K. (2009). Nonlocal elasticity theory for vibration of nanoplates. Journal of Sound and Vibration 325: 206 – 223.

Ruud J.A., Jervis T.R., Spaepan F. (1994). Nanoindention of Ag/Ni multilayered thin films. Journal. Applied. Physics 75: 4969.

Reddy J.N. (2007). Nonlocal theories for bending, buckling and vibration of beams. International Journal Engineering Science 45: 288-307.

Ru C.Q. (2001). Axially compressed buckling of a doublewalled carbon nanotube embedded in an elastic medium. Journal Mechanic Physic Solids 49: 1265–1279.

Shen H., Zhang C.L. (2010). Torsional buckling and postbuckling of double-walled carbon nanotubes by nonlocal shear deformable shell model. Composite Structure 92:1073–84.

Wang C. M., Duan W.H. (2008). Free vibration of nanorings/arches based on nonlocal elasticity. Journal Applied Physics 104: 014303.

Wang Q., Wang C.M. (2007). The constitutive relation and small scale parameter of nonlocal continuum mechanics for modelling carbon nanotubes. Nanotechnology 18: 7:075702.

Wong E.W., Sheehan P.E., Lieber C.M. (1997). Nanobeam mechanics: elasticity, strength, and toughness of nanorods and nanotubes. Science 277: 1971–1975.

Wu J.X., Li X.F., Tang G.J. (2011). Bending wave propagation of carbon nanotubes in a bi-parameter elastic matrix. Physica B: Condensed Matter 407: 684-688.

Yang F., Chong A.C.M., Lam D.C.C., Tong P. (2002). Couple stress based strain gradient theory for elasticity. International Journal of Solids Structure 39: 2731-2743.

Yoon J., Ru C.Q., Mioduchowski A. (2003). Vibration of an embedded multiwall carbon nanotube. Computational Science Technology 63: 1533–1542.

Zhang Y. Q., Liu X., Liu G.R. (2007).Thermal effect on transverse vibrations of double-walled carbon nanotubes. Nanotechnology 18: 445701.

Zhou S.J., Li Z.Q. (2001). Metabolic response of Platynota stultana pupae during and after extended exposure to elevated CO2 and reduced O2 atmospheres. Shandong University Technology 31: 401-409.